An Adventure in Space (Group) and (Reaction) Time: Divergent Synthesis of Heterobimetallic Complexes of Zinc with Lewis Acids

Thesis by:

Shaun R. Kelsey

In Partial Fulfillment of the Requirements for the Degree of
Bachelor of Science with Honors in Chemistry

Lawrence, Kansas
May 2019

Acknowledgements

To my wife, Ashley. Thank you for always being there and supporting me. It's been an amazing adventure with you over the last 14 years. You never seem to be surprised at what I come up with, even when I told you I wanted to leave the Army go spend the better part of the next decade in college again. I know the last two years haven't been that fun, with many late nights spent on campus, but you have always been understanding (if not always happy 😊). Without you, I would have not been able to make it through these last two years with any sense of sanity. You are my better half that always keeps me grounded. I love you. (Tie!)

To my mom, dad, and siblings; it has been amazing being back in Kansas and being able to see you guys on a regular basis. Moving away for my first iteration of college was hard, but I am thankful that my second iteration has brought me back. I know that it never seems like we see each other enough, but that fact that I am close enough to come to birthdays, holidays, and just random get-togethers means the world to me. I love you guys.

To my mentor, Prof. James Blakemore; I would like to express my deep appreciation for allowing me to join your research group. I know that it was a risk letting a student into the group who hadn't been in a classroom since before many of the group members were even in college. Since joining, you have always pushed me to achieve as much as I could. Without your guidance, teaching, and endless, boundless, tireless (seriously, when do you sleep?) energy to always do better, I would not have ended this undergraduate experience where I am.

To Davide, thank you for the numerous hours of conversation and teaching. I learned very quickly that you love to teach and pass on knowledge, and it was a pleasure to be taught by you. Your future students are lucky to have you, and I can't wait to see what Prof. Lionetti does with his future group.

To Amit Kumar, thank you for being my friend, mentor, and workout partner. Because of you, I am in better shape (Ashley appreciates that too), a better volleyball player, and a better chemist. Thank you for showing me that there is more to being a graduate student than living in the lab.

To Katie Johnson, thank you for being my mentor. You had the unfortunate duty of taking a fumbling undergrad who knew nothing about the lab and making him into a chemist. I hope the next step of your journey is everything you want. You will be missed in the lab.

To the rest of the Blakemore group, you have all been like my family. We have had highs and lows, but we all support each other. I look forward to starting my graduate career with you all next year.

To the people that help me make sense of what I prepare in the lab. To Victor Day, our amazing crystallographer and my personal spirit animal; Sarah Neuenswander and Justin Douglas, our amazing NMR team. Without you, none of us would be able to do our job. You are incredibly hard working and I appreciate everything you do.

Abstract

Assembly of heterobimetallic complexes is challenging due to the propensity of ditopic ligands to bind metals unselectively. This challenge is exacerbated in situations in which two redox-inactive metals are to be coordinated within one ligand framework, as such metals can bind in a variety of coordination environments. In this thesis, the preparation and isolation of four heterobimetallic complexes of zinc, a redox-inactive first-row transition metal, with a range of other redox-inactive Lewis acidic metals (Na^{+}, Ca^{2+}, Nd^{3+}, and Y^{3+}) are reported. The complexes were prepared via a divergent route in which a common monometallic zinc complex featuring a crown-ether-like site within a macrocyclic structure was selectively metallated with triflate salts of sodium, calcium, neodymium, and yttrium. One-dimensional ^{1}H and two-dimensional $^{1}H–^{1}H$ Correlation Spectroscopy (COSY) Nuclear Magnetic Resonance (NMR) studies provide robust support for synthesis of the target heterobimetallic compounds. Single crystals suitable for X-ray diffraction analysis were grown of the [Zn,Nd] complex, revealing the expected atomic connectivity within the macrocyclic framework. In the solid state, the zinc center is five-coordinate, with a terminal acetonitrile ligand; this finding contrasts with the structure of the analogous [Ni,Nd] complex that instead features a four-coordinate nickel center. These results are discussed in the context of developing model compounds for study of the spectroscopic and electrochemical properties of heterobimetallic complexes containing redox-inactive Lewis acids.

Introduction

"*Look deep into nature, and then you will understand everything better.*" - Albert Einstein

While Dr. Einstein may not have guessed that one of his quotes would be redirected to the opening line of an undergraduate thesis, it remains quite appropriate for this topic. Over the last four billion years of practice, Nature has found solutions to problems that we as humans are only now coming to appreciate. An example of this skill is Nature's design and utilization of enzymes, which are capable of catalyzing complex reactions with an efficiency that chemists strive to match.[1]

Of particular interest are those enzymes with active sites that contain multiple, different metals, as these enzymes seem to possess unique properties that are inaccessible in simpler, homomultimetallic analogues. These properties include enhanced catalytic activity, improved stability, and increased binding affinity for the substrate.[2-5] In addition, while there are only a few characterized enzymes in this class, the reactions that they catalyze are at the forefront of contemporary research in biological and inorganic chemistry. These important reactions include water oxidation, nitrogen reduction/fixation, and O_2 reduction; and due to their applications in sustainability science and development of renewable energy, understanding the mechanisms of these reactions and how enzymes can carry them out attracts great attention.[6-8]

A common feature in many of these enzymes is the presence of a redox-inactive (at physiologically-relevant potentials) metal bound in close proximity to other, redox-active metal(s).[6-8] However, the effect that this redox-inactive metal has on the overall properties and reactivity of the multimetallic complex is not well understood. Perhaps the most famous example of this ambiguity is the oxygen evolving complex (OEC) of Photosystem II. At heart of this

complex is a cubane-type cluster consisting of four manganese atoms and a calcium atom, all linked together by oxygen atoms which serve as oxo bridges.[8] This catalytic Mn_4CaO_n cluster (n changes depending on the mechanistic proposal and specific intermediate being discussed) utilizes electron transfer reactions to split H_2O into molecular oxygen, protons, and electrons according to the reaction below[8]:

$$2H_2O \rightarrow O_2 + 4H^+ + 4e^- \quad (1)$$

It has been shown that the redox-inactive Ca^{2+} ion is crucial in order for this complex to remain catalytically active, yet the reasons for this are unclear.[9-10] In addition, while a limited number of dication-substituted OEC complexes such Mn_4SrO_5 remain catalytically active; others such as Mn_4CdO_5 do not.[11] This indicates that while the charge of the redox-inactive ion plays a role, this is not the only contributing factor. It has been postulated, however, that the Lewis acidity of the redox-inactive metal could also play a major role in catalytic activity of these complexes.[10-13]

Thus, to improve the design of artificial catalysts, an important and outstanding goal remains in understanding what role this metal plays in the catalytic process. In order to do this, some researchers have synthesized model complexes that are able to act as analogues for these heterometallic active sites. For example, synthetic analogues of the OEC containing four or more metal ions have been synthesized in order to understand the role of the calcium ion in this enxyme.[14-17] However, these complexes have some steep drawbacks, including that they are synthetically challenging to prepare, unstable at room temperature, and are difficult to custom tailor for new applications.

An alternate approach which has been taken by our group and others centers on use of a simpler, heteroditopic ligand framework that incorporates distinct binding motifs that allow for

orthogonal metalation.[2] Such frameworks can be used to systematically study the role that Lewis-acidic metals have in heterobimetallic complexes by comparing the properties of the monometallic complex to that of the species that incorporate Lewis acidic cations. Ligands of this type are known in literature, and more specifically, the heteroditopic macrocyclic ligand introduced by Reinhoudt and co-workers is the topic of this paper.[18] This ligand framework features a Schiff base, salophen cavity which can be used to incorporate first-row transition metals with a nearby crown-ether-like moiety used for installing Lewis-acids.[19-20]

Recently, this ligand has been utilized by Kumar and co-workers in our group to study the effects that trivalent Lewis acids have on the electronic properties and stability of heterobimetallic complexes of nickel.[21] In this published work, electrochemical studies were conducted using cyclic voltammetry to determine the shift of the reduction potential of the nickel complexes as a function of the Lewis acidity of the redox-inactive metal.[21] The observed reductions in this work were postulated to be metal-centered, rather than ligand-centered. However, as the reductions of the nickel complexes were determined by cyclic voltammetry to be chemically and electrochemically irreversible, ambiguity remains as to the localization of the reduction event in question. This thesis is aimed at synthesizing zinc-containing analogues of these nickel complexes that could be used to further investigate this theory. Specifically, the d^8 nickel(II) center in the salophen cavity was substituted with zinc(II), a d^{10} transition metal that has a much more negative reduction potential and therefore can be considered to be redox inactive.[22] This thesis lays out the synthetic chemistry and isolation of the target heterobimetallic complexes of zinc with a tunable range of Lewis acids (Na^+, Ca^{2+}, Nd^{3+}, and Y^{3+}). Notably, Reinhoudt and co-workers demonstrated synthesis of the monometallic zinc complex in prior work. However, preparation of the heterobimetallic zinc complexes or electrochemical work have not been carried out previously. In future work, we will

investigate whether the complexes are indeed redox inactive at the potentials associated with the reduction of the nickel complexes; pending this result, we will be well poised to quantify the role of a Lewis acidic metal on the reduction potential of a redox-active ligand, as well as highlight unique features in the chemistry by comparison to the nickel analogues.

Ligand Design

The key features of our ligand design are highlighted in Figure 1 below:

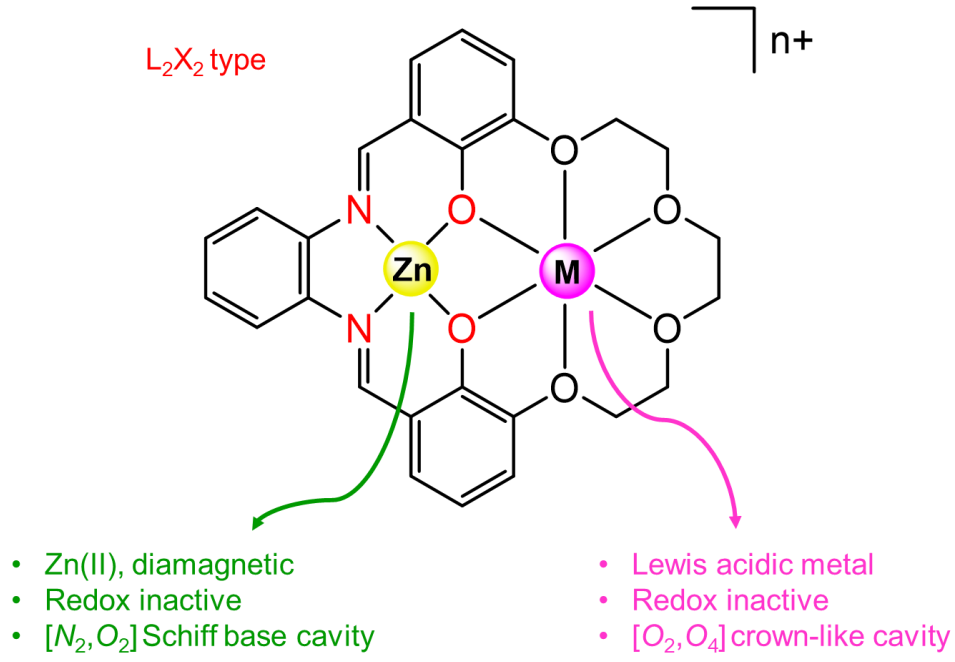

Figure 1. Features of the ditopic ligand framework.

This ligand design features the same modular capability as that utilized by Kumar and coworkers.[20] The design features two separate binding sites: the [N_2,O_2] site for the binding of the zinc ion, and the [O_2,O_6] crown-ether site for the incorporation of a broad range of Lewis acids. Zinc(II) was chosen due to its quite negative reduction potential compared to nickel(II). The Lewis acids that were utilized in the synthetic chemistry were triflate salts of sodium, calcium, neodymium, and yttrium. The pK_a values associated with each of the corresponding metal ions (determined from

the aqua complexes) are: sodium (pK_a = 14.7), calcium (pK_a = 12.7), neodymium (pK_a = 9.0), and yttrium (pK_a = 8.3).[20] These Lewis acids were chosen as they span a broad range of over six orders of magnitude of Lewis acidity.

Divergent Synthesis

Methods

All solvents used were commercial grade and dried using a Pure Process Technology LLC Glass Contour solvent system or by manual manipulations with 4 Å molecular sieves. 2,3-Dihydroxybenzaldehyde (97%, Alfa Aesar) was purified via sublimation prior to use. Sodium hydride (60% dispersion in mineral oil, Sigma) was washed under inert atmosphere with hexanes prior to use. Triethylene glycol ditosylate was dried at 30°C under vacuum for 24 hours prior to use.

Synthesis of 3,3´-(3,6-Dioxaoctane-1,8-diyldioxy)bis(2-hydroxybenzaldehyde)

The synthesis of this polyether precursor was adapted from literature according to the reaction scheme in Scheme 1.[17]

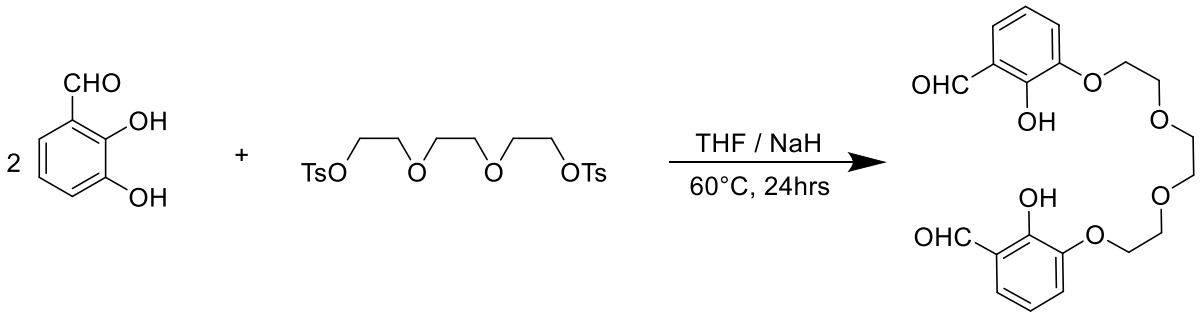

Scheme 1. Synthetic scheme for 3,3´-(3,6-Dioxaoctane-1,8-diyldioxy)bis(2-hydroxybenzaldehyde)

In detail, our procedure is as follows: To a dry Schlenk flask equipped with a stir bar, NaH (0.528 g, 22.0 mmol) in 5 mL of dry THF was added under an inert atmosphere. To this suspension,

2,3-dihydroxybenzaldehyde (1.39 g, 10.0 mmol) dissolved in 5 mL of dry THF was slowly transferred via cannula over the course of 30 minutes while keeping the temperature of the reaction below 25 ºC. Upon complete addition of the 2,3-dihydroxybenzaldehyde, the solution was allowed to stir for 1 hour. To this, triethylene glycol ditosylate (2.30 g, 5.00 mmol) dissolved in 5 mL of THF was added in one portion via a syringe and the resulting mixture was stirred for 24 hours under inert atmosphere. This solution was quenched with 60 mL of deionized water, to afford a dark brown solution which was extracted with 2 x 60 mL portions of $CHCl_3$ to remove any unreacted triethylene glycol ditosylate. The organic layer was discarded and the aqueous layer was acidified to a pH of 1 with 6 M HCl. This mixture was then extracted with 3 x 10 mL portions of $CHCl_3$. The aqueous layer was discarded and the organic layers were combined, washed with 1 M aqueous HCl, and dried over anhydrous $MgSO_4$. The solvent was removed under reduced pressure. Purification was accomplished using column chromatography with a silica gel stationary phase and $CHCl_3$ as the eluent. Yield: 38% (742 mg, 1.9 mmol).

Synthesis of H_2L-Ba

The synthesis of a macrocyclic barium-containing complex en route to the zinc monometallic complex was adapted from literature according to the reaction scheme below:[17]

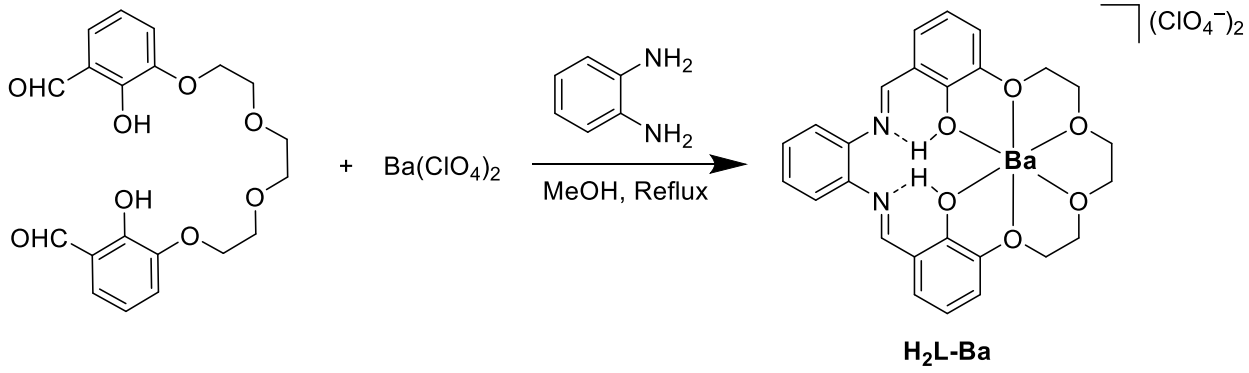

H_2L-Ba

Scheme 2. Synthetic Scheme for **H_2L-Ba**.

$Ba(ClO_4)_2$ (172 mg, 0.512 mmol) was added to a dry, three-neck round-bottom flask under inert atmosphere with 50 mL of dry, degassed MeOH (0.01 M). The flask was heated to reflux and the reaction mixture was stirred until complete dissolution of the $Ba(ClO_4)_2$ was observed. To the refluxing solution 1 equivalent of 3,3´-(3,6-Dioxaoctane-1,8-diyldioxy)bis(2-hydroxybenzaldehyde) (200 mg, 0.512 mol) dissolved in 5 mL of THF was slowly added. Over the course of the next hour, 1,2-phenylenediamine (55.4 mg, 0.512 mmol) in 5 mL of dry, degassed MeOH (0.1 M) was added. Upon complete addition, the solution had been allowed to stir for another 30 minutes before being cooled to room temperature. After cooling, the resulting orange precipitate was filtered and washed with ice-cold methanol. Yield: 52% (213 mg, 26.7 mmol).

Synthesis of L-Zn

Synthesis of the monometallic zinc complex **L-Zn** was adapted from literature according to the reaction in Scheme 3:[17]

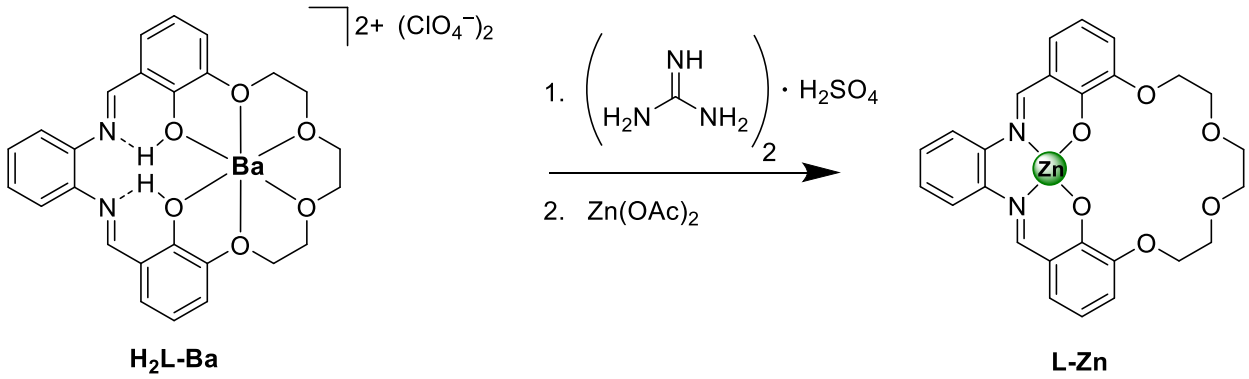

Scheme 3. Synthetic scheme for **L-Zn**.

Guanidium sulfate (116 mg, 0.54 mmol) dissolved in 25 mL of water was added to a suspension of **H2L-Ba** (208 mg, 0.26 mmol) in 25 mL $CHCl_3$. This solution was stirred for 4 hours until the organic layer was clear. The organic layer was separated and diluted with 15mL of MeOH. To this solution, 1 equivalent of $Zn(OAc)_2$ in 5mL of MeOH was added and the resulting mixture was

stirred for 1 hour. The product was crashed out with ether, filtered and washed with cold $CHCl_3$. Yield: 85% (130 mg, 0.22 mmol).

Synthesis of L-Zn-M (M = Na, Ca, Nd, or Y)

Synthesis of the heterobimetallic **L-Zn-M** (**M = Na, Ca, Nd, or Y)** complexes was adapted from literature according to the reaction scheme below:[17]

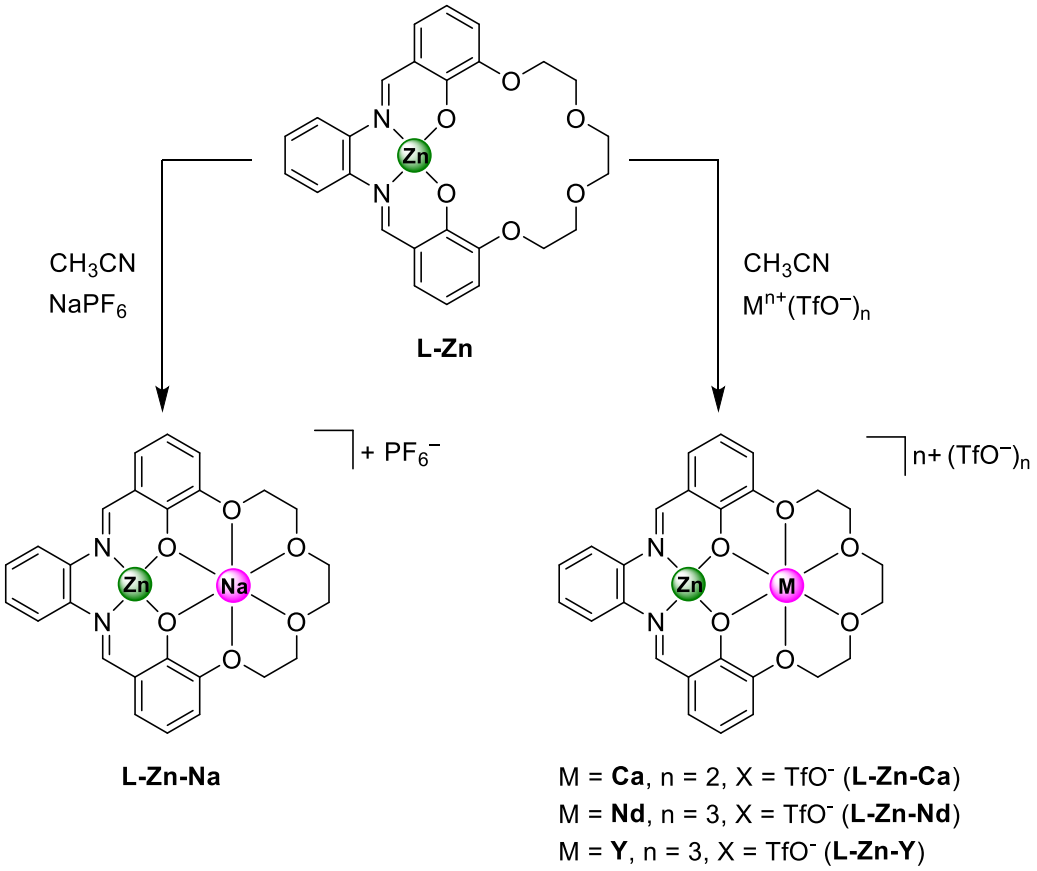

Scheme 4. Divergent synthetic strategy for preparation of heterobimetallic complexes of zinc.

L-Zn (80mg, 0.152mmol) was added to a 50mL Schlenk flask with 12mL of acetonitrile under inert atmosphere. One equivalent of the desired metal salt [$NaPF_6$, $Ca(TfO)_2$, $Nd(TfO)_3$, $Y(TfO)_3$] dissolved in 12mL of acetonitrile was slowly added to this heterogenous solution. The resulting mixture was stirred for one hour, during which the color of the solution changed from dark yellow

to a lighter yellow. The extent of the color change was dependent on the Lewis acidity of the metal added. The higher the Lewis acidity, the lighter the resulting solution became. Solvent was evaporated under vacuum. Yield: 87% (112 mg – 168 mg depending on metal salt used, 0.132 mmol).

Characterization

Nuclear Magnetic Resonance

Nuclear magnetic resonance (NMR) spectroscopic studies of **L-Zn** (Figure 2) confirm the structure of the desired compound. The ^{1}H-NMR spectrum shows a singlet at 9.03 ppm (**7**) that corresponds to the imine proton of the ligand (s, 2H), and a triplet at 6.43 ppm (**5**) that corresponds to the *ortho* protons of the outer phenyl rings (t, 2H). In addition, in the aromatic region the spectrum shows two multiplets at 7.93 ppm and 7.39 ppm (m, 2H each) which correspond to the protons on the salophen ring (**8, 9**) as well as two doublets at 7.05 ppm and 6.86 ppm (d, 2H each) that correspond to the outer phenyl rings that surround the salophen cavity (**4, 6**). We also observe three singlets (s, 4H each) in the aliphatic region that correspond to the protons of the the crown-ether cavity (**1-3**).

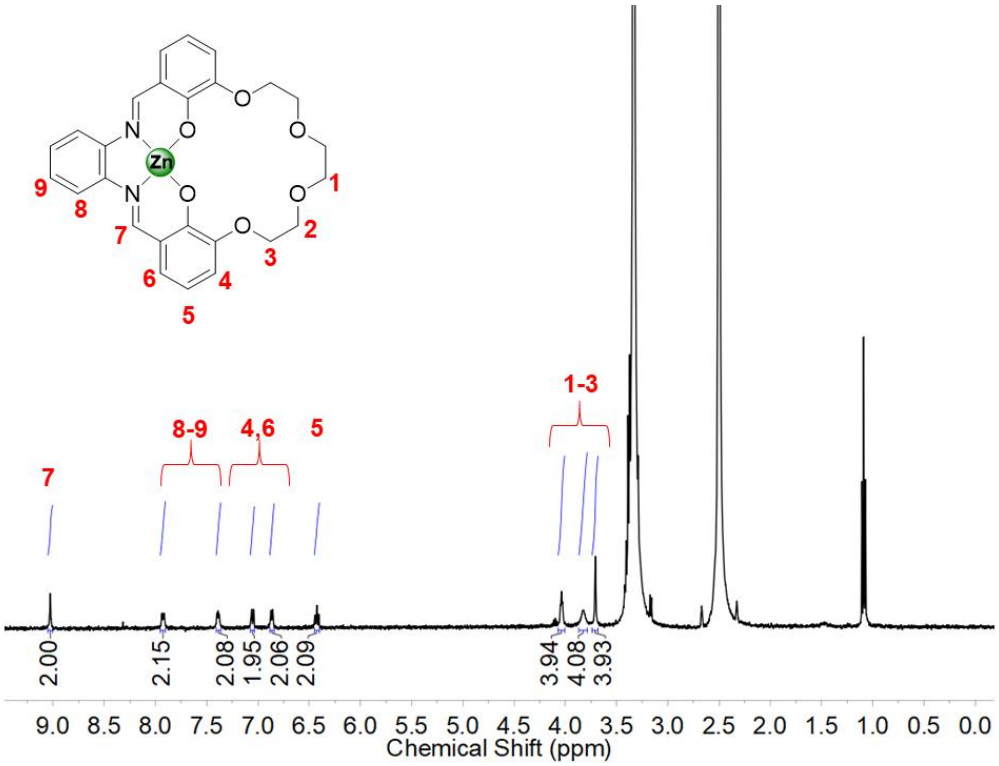

Figure 2. ^{1}H NMR (500 MHz, DMSO) Spectra of **L-Zn** with the protons labeled and peaks integrated. Non-integrated peaks correspond to residual solvent signals.

Assignment of the aromatic region peaks was accomplished using 2D Correlation Spectroscopy (COSY) NMR seen in Figure 3.

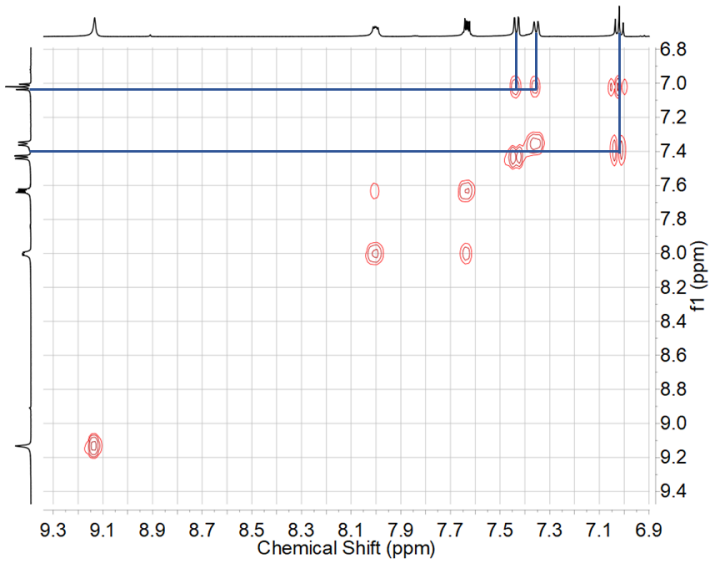

Figure 3. 2D COSY for **L-Zn** showing the correlation of the triplet at 6.43 ppm (**5**) that corresponds to the *ortho* protons of the outer phenyl rings to the two that correspond to the outer phenyl rings that surround the salophen cavity (**4, 6**).

^{1}H NMR was also used to verify the structure of the **L-Zn-M** complexes (M = Na, Ca, Nd, and Y) which can be seen in Figures 4-7 below. The NMR spectra are plotted in Figures 4-7 in order of the derivative with the least Lewis acidic cation (Na^{+}, Figure 4) to most (Y^{3+}, Figure 7). The peak integrations and splitting of each diamagnetic complex is consistent with that of the **L-Zn** ligand. However, due to the paramagnetic nature of the **L-Zn-Nd** complex (Figure 6) there are no discernible splitting patterns for the observed resonances. Furthermore, integrations were not calculated or interpreted for the observed resonances; due to the presence of the three unpaired electrons on the neodymium center, faster-than-usual and unpredictable proton relaxations are expected in this case, distorting integration values and interfering with typical splitting patterns. Generally, however, an interesting trend emerges from the NMR studies: the peak signals become more deshieleded as the Lewis acidity of the redox-inactive metal increases.

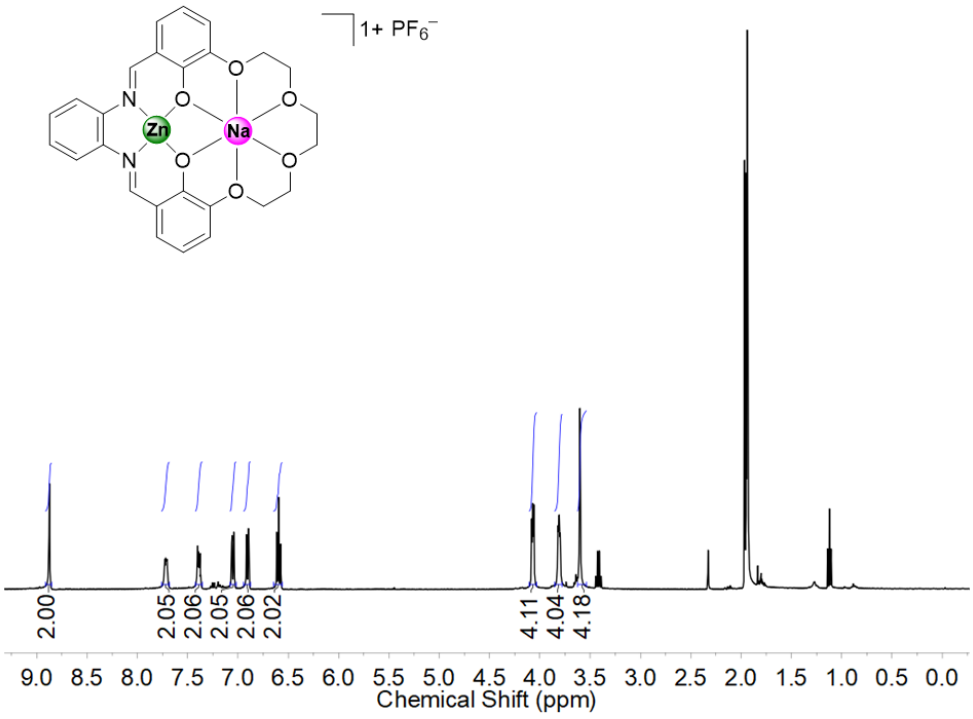

Figure 4. ^{1}H NMR (500 MHz, MeCN) Spectra of **L-Zn-Na** with the peaks integrated. Non-integrated peaks correspond to residual solvent signals.

The ^{1}H-NMR spectrum of **L-Zn-Na** shows a singlet at 8.87 ppm that corresponds to the imine proton of the ligand (s, 2H); two multiplets at 7.72 ppm and 7.39 ppm (m, 2H each) which correspond to the protons on the salophen ring (**8, 9**); two doublets at 7.05 ppm and 6.90 ppm (d, 2H each) that correspond to the outer phenyl rings that surround the salophen cavity (**4, 6**); a triplet at 6.59 ppm (**5**) that corresponds to the *ortho* protons of the outer phenyl rings (t, 2H); and three singlets at 4.07 ppm, 3.87 ppm, and 3.60 ppm (s, 4H each) in the aliphatic region that correspond to the protons of the the crown-ether-like cavity (**1-3**).

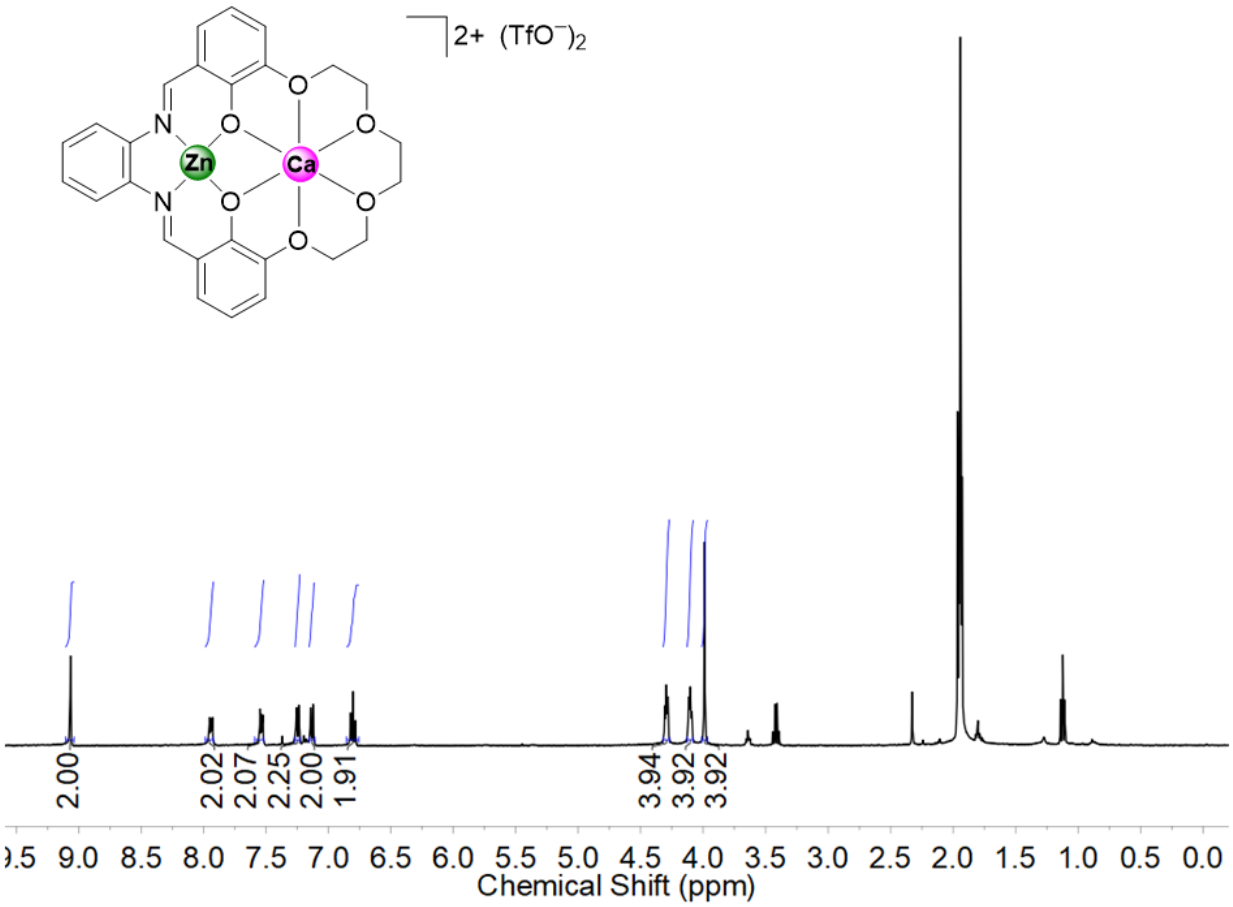

Figure 5. ^{1}H NMR (500 MHz, MeCN) Spectra of **L-Zn-Ca** with the peaks integrated. Non-integrated peaks correspond to residual solvent signals.

The ^{1}H-NMR spectrum of **L-Zn-Ca** shows a singlet at 9.07 ppm that corresponds to the imine proton of the ligand (s, 2H); two multiplets at 7.94 ppm and 7.54 ppm (m, 2H each) which correspond to the protons on the salophen ring (**8, 9**); two doublets at 7.25 ppm and 7.13 ppm (d, 2H each) that correspond to the outer phenyl rings that surround the salophen cavity (**4, 6**); a triplet at 6.80 ppm (**5**) that corresponds to the *ortho* protons of the outer phenyl rings (t, 2H); and three singlets at 4.30 ppm, 4.11 ppm, and 3.99 ppm (s, 4H each) in the aliphatic region that correspond to the protons of the the crown-ether-like cavity (**1-3**).

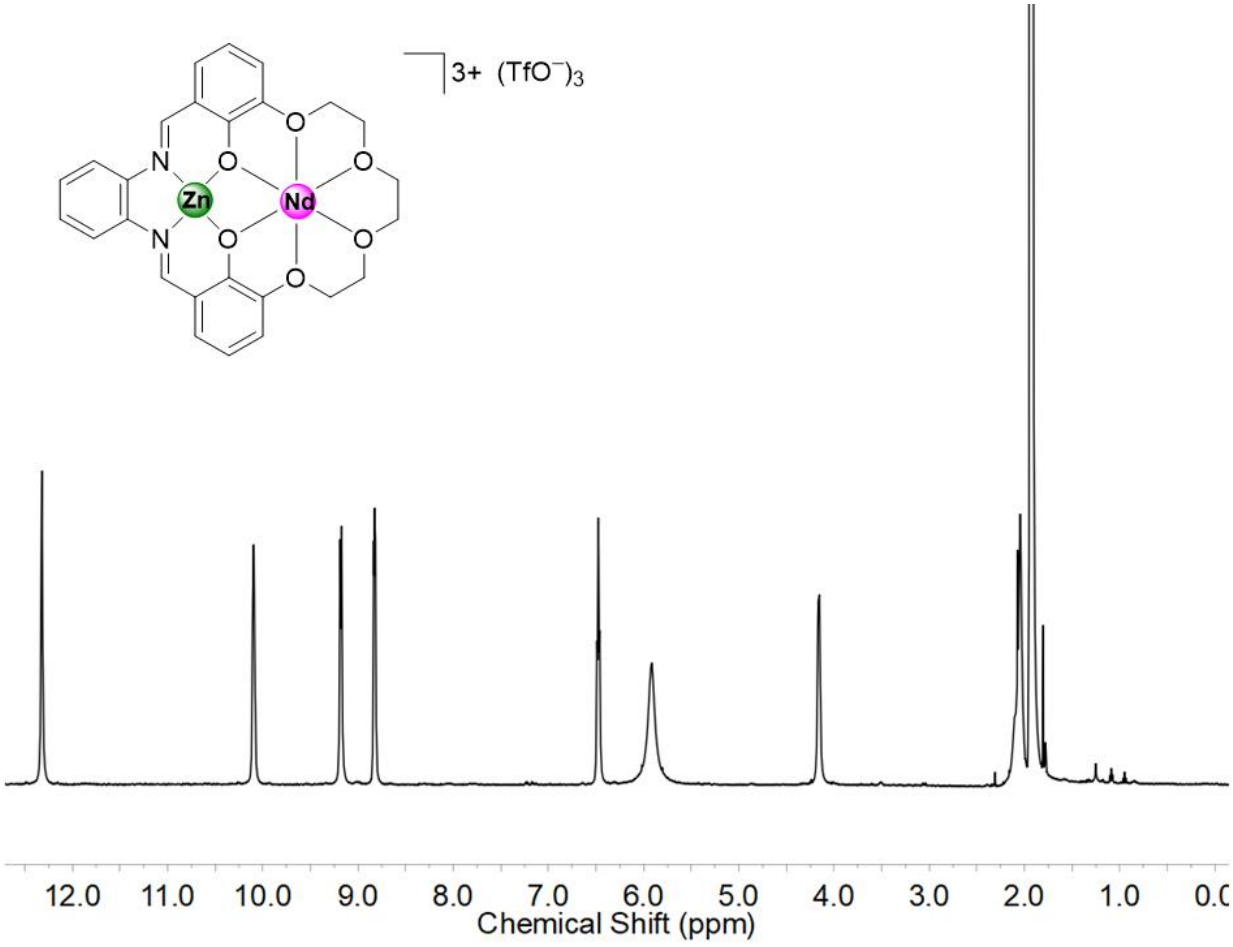

Figure 6. ^{1}H NMR (500 MHz, MeCN) Spectra of **L-Zn-Nd**. Non-integrated peaks correspond to residual solvent signals.

Nine unique resonances were expected for NMR spectrum associated with the sample of **L-Zn-Nd**. However, due to the paramagnetic nature of this complex, only seven peaks are present that are shifted significantly from the case of the other complexes in the series. This could be due to the proximity of some of the crown-ether-like protons to the paramagnetic Nd, which could cause these resonances to become undetectable under these conditions or overlap with other resonances.

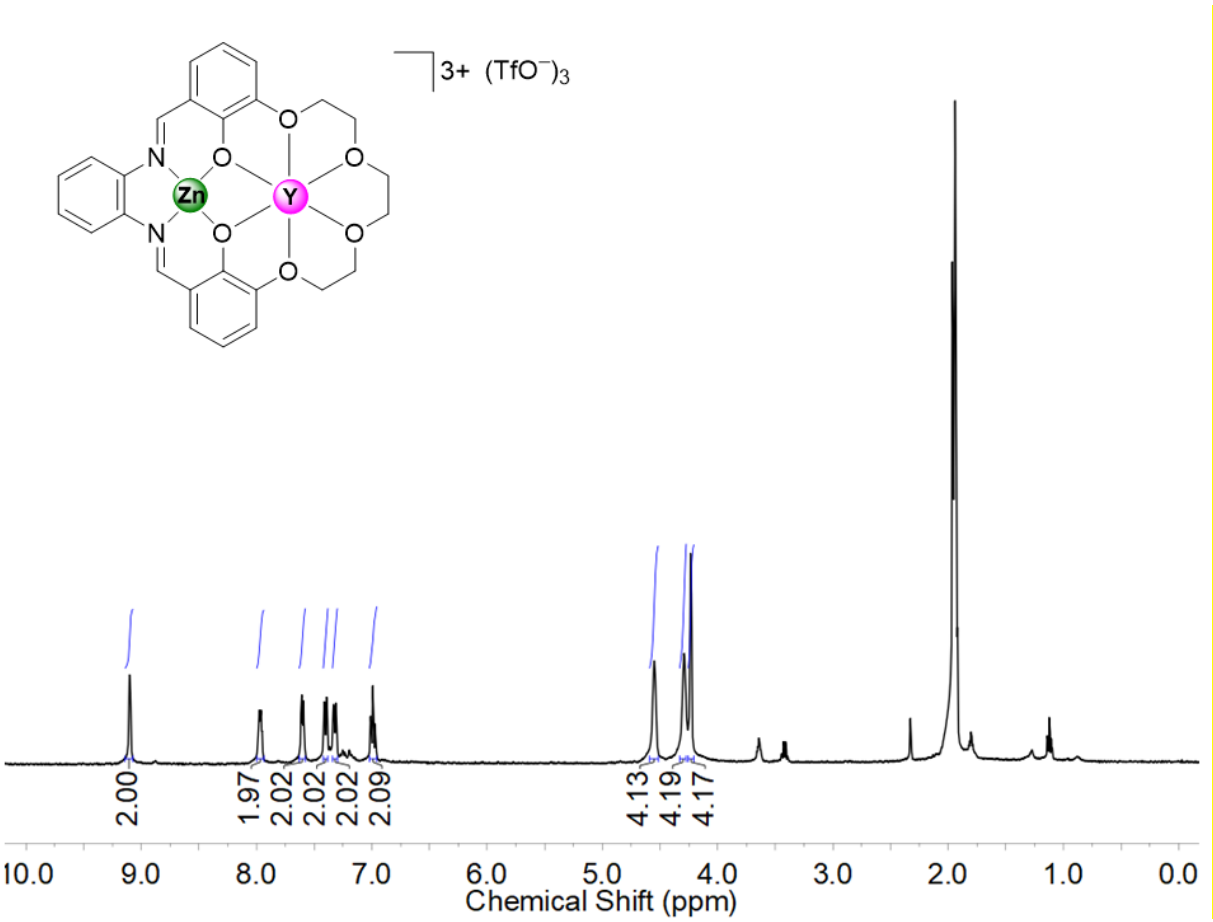

Figure 7. ^{1}H NMR (500 MHz, MeCN) Spectra of **L-Zn-Y**. Non-integrated peaks correspond to residual solvent signals.

The ^{1}H-NMR spectrum of **L-Zn-Y** shows a singlet at 9.10 ppm that corresponds to the imine proton of the ligand (s, 2H); two multiplets at 7.97 ppm and 7.60 ppm (m, 2H each) which correspond to the protons on the salophen ring (**8, 9**); two doublets at 7.40 ppm and 7.32 ppm (d, 2H each) that correspond to the outer phenyl rings that surround the salophen cavity (**4, 6**); a triplet at 6.99 ppm (**5**) that corresponds to the *ortho* protons of the outer phenyl rings (t, 2H); and three singlets at 4.55 ppm, 4.29 ppm, and 4.23 ppm (s, 4H each) in the aliphatic region that correspond to the protons of the the crown-ether-like cavity (**1-3**).

Single-Crystal X-Ray Diffraction Studies

The following section is based upon preliminary structural data obtained for **L-Zn-Nd**. Crystals suitable for X-ray diffraction were obtained by vapor diffusion of diethyl ether into acetonitrile under inert atmosphere. Crystals were needle-like in morphology with a triclinic crystal system. The Zn center is coordinated to the [N_2,O_2] cavity and an acetonitrile molecule in a distorted square pyramidal-like geometry while the Nd metal center is coordinated to the [O_2,O_6] cavity and three triflate molecules. In solution, **L-Zn-Nd** possesses a C_s geometry, but in the solid-state is C_1 due to the protrusion of the zinc out of the plane of the molecule and the non-symmetric bend to the crown-ether-like cavity. These features can be seen in Figure 8, along with a side-by-side comparison of the **L-Ni-Nd** complex synthesized by Kumar and coworkers.[21]

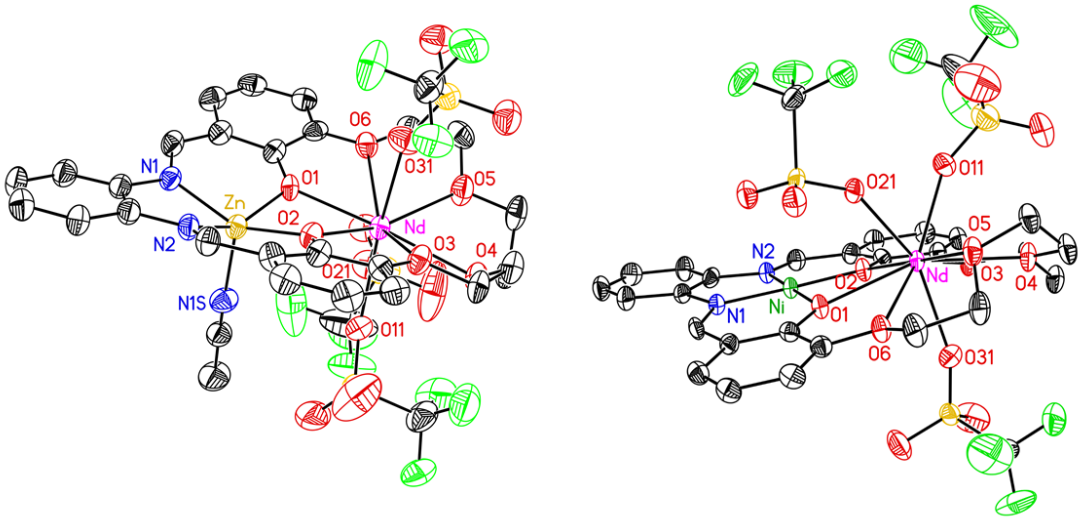

Figure 8. Crystal structure comparison of the preliminary **L-Zn-Nd** structure and its nickel analogue obtained using X-ray diffraction. Displacement ellipsoids shown at 50% probability.

One of the most interesting features of **L-Zn-Nd** is that in the solid state the zinc center is five-coordinate, with a terminal acetonitrile ligand, which contrasts sharply with the structure of the analogous [Ni,Nd] complex that instead features a four-coordinate nickel center. In addition, there is a noticeable difference in the bond distances between the Zn and Ni metals and their respective

[N_2,O_2] cavities. Specifically, the distances between Zn(II) and its cavity are all longer than the Ni(II) analog, as can be seen in Table 1. This is most likely due to the fact that while Zn(II) and Ni(II) are in the same oxidation state, the fifth ligand of Zn results in it being less electron-deficient and needing to pull less density from the [N_2,O_2] cavity. Also, the fifth ligand causes geometric distortion of the cavity (the protrusion of the Zn from the plane of the ligand), which also influences the longer bond distances.

Table 1. Important bond length comparisons between **L-Zn-Nd** and **L-Ni-Nd**.

Bond	**L-Zn-Nd**	**L-Ni-Nd**
M•••M'	3.478(1)	3.505(1)
M–N1	2.024(7)	1.855(3)
M–N2	2.038(7)	1.853(3)
M–O1	2.004(6)	1.859(3)
M–O2	1.994(6)	1.856(2)
M'–O1	2.386(6)	2.425(2)
M'–O2	2.410(6)	2.490(3)
M'–O3	2.661(6)	2.703(3)
M'–O4	2.576(6)	2.579(3)
M'–O5	2.594(7)	2.575(3)
M'–O6	2.706(6)	2.611(3)
C=N1	1.303(12)	1.298(5)
C=N2	1.279(12)	1.298(5)

Finally, a comparison of the crystal data and structural refinement information between the preliminary **L-Zn-Nd** structure and **L-Ni-Nd** can be found in Table 2 on the next page. As you will see, there is a relatively large Q-peak of 6.38 e/Å^3 which we believe is the result of a distorted triflate.

Table 2. Crystal data and structure refinement for **L-Zn-Nd** and its analog, **L-Ni-Nd**.

	L-Zn-Nd	**L-Ni-Nd**
KU Identification Code	v21e	q31g
Empirical formula	$C_{33}H_{24}F_9N_4NdO_{15}S_3Zn$	$C_{29}H_{24}F_9N_2NdNiO_{15}S_3$
Formula weight	1193.35	1110.63
Temperature/K	199.99	296.15
Crystal system	triclinic	triclinic
Space group	P-1	P-1
a/Å	12.2410(5)	10.7125(11)
b/Å	13.3353(5)	11.7563(14)
c/Å	14.9569(6)	16.1835(17)
α/°	74.2649(14)	81.781(7)
β/°	71.9890(14)	81.228(7)
γ/°	72.1764(14)	69.173(7)
Volume/Å^3	2168.01(15)	1874.0(4)
Z	2	2
ρ_{calc}g/cm^3	1.828	1.968
μ/mm^{-1}	12.059	13.712
F(000)	1178	1098
Crystal size/mm^3	0.4 × 0.1 × 0.065	0.03 × 0.02 × 0.02
Radiation	CuKα (λ = 1.54178)	CuKα (λ = 1.54178)
2Θ range for data collection/°	6.336 to 136.808	5.55 to 141.012
Index ranges	$-14 \le h \le 14$, $-15 \le k \le 15$, $-17 \le l \le 14$	$-12 \le h \le 11$, $-14 \le k \le 14$, $-19 \le l \le 18$
Reflections collected	23498	47771
Independent reflections	7587 [R_{int} = 0.0630, R_{sigma} = 0.0646]	6655 [R_{int} = 0.0603, R_{sigma} = 0.0330]
Data/restraints/parameters	7587/0/595	6655/0/541
Goodness-of-fit on F^2	1.049	1.072
Final R indexes [I>=2σ (I)]	R1 = 0.0786, wR2 = 0.2151	R1 = 0.0408, wR2 = 0.1044
Final R indexes [all data]	R1 = 0.0840, wR2 = 0.2251	R1 = 0.0437, wR2 = 0.1062
Largest diff peak/hole / e Å^{-3}	6.38/-2.02	2.65/-1.29
Empirical formula	$C_{33}H_{24}F_9N_4NdO_{15}S_3Zn$	$C_{29}H_{24}F_9N_2NdNiO_{15}S_3$

Conclusion

In this thesis, the synthesis and characterization of four heterobimetallic complexes of zinc, with a range of other redox-inactive Lewis acidic metals (Na^{+}, Ca^{2+}, Nd^{3+}, and Y^{3+}) are reported. These complexes were developed for utilization as model compounds in studies of the spectroscopic and electrochemical properties of heterobimetallic complexes containing redox-inactive Lewis acids. The complexes feature a Schiff-base-type [N_2,O_2] cavity for the binding of the zinc as well as a crown-ether-like [O_2,O_6] site within the macrocyclic structure for selective metalation with triflate salts of sodium, calcium, neodymium, and yttrium. Characterization was accomplished via one-dimensional ^{1}H and two-dimensional ^{1}H–^{1}H Correlation Spectroscopy (COSY) NMR studies. Single crystals suitable for X-ray diffraction analysis were grown of the [Zn,Nd] complex, and the data show that the zinc center is five-coordinate in the solid state and contrasts with the analogous [Ni,Nd] complex that features a four-coordinate nickel center. Finally, and of particular note, while a variety of O-atom bridged [Zn,Nd] complexes have been synthesized prior to this work, the reported **L-Zn-Nd** is the first macrocyclic complex of its type to be synthesized and crystallographically characterized.[23]

References

1. Sawaya, M.; Kraut, J. Loop and subdomain movements in the mechanism of Escherichia coli dihydrofolate reductase: crystallographic evidence. *Biochemistry*. **1997**, 36, 586-603.

2. Gavrilova, A.; Bosnich, B. Principles of Mononucleating and Binucleating Ligand Design. *Chem. Rev*. **2004**, 104, 349-383.

3. Buchwalter, P.; Rose, J.; Braunstein, P. Multimetallic Catalysis Based on Heterometallic Complexes and Clusters. *Chem. Rev*. **2015**, 115, 28-126.

4. Ogo, S.; Kabe, R.; Uehara, K.; Kure, B.; Nishimura, T.; Menon, S.C.; Harada, R.; Fukuzumi, S.; Higuchi, Y.; Ohhara, T.; Tamada, T.; Kuroki, R. A dinuclear Ni(μ-H)Ru complex derived from H_2. *Science*. **2007**, 316, 585-587.

5. Kure, B.; Sano, M.; Nakajima, T.; Tanase, T. Systematic Heterodinuclear Complexes with MM′(μ-meppp) Centers That Tune the Properties of a Nesting Hydride (M = Ni, Pd, Pt; M′ = Rh, Ir; H_2meppp = meso-1,3-Bis[(mercaptoethyl)phenylphosphino]propane). *Organometallics*. **2014**, 33, 3950-3965.

6. Tsukihara, T.; Shimokata, K.; Katayama, Y.; Shimada, H.; Muramoto, K.; Aoyoma, H.; Mochizuki, M.; Shinzawa-Itoh, K.; Yamashita, E.; Yao, M.; Ishimura, Y.; Yoshikawa, S. The low-spin heme of cytochrome c oxidase as the driving element of the proton-pumping process. *Proc. Natl. Acad. Sci. USA.* **2003**, *100*, 15304.

7. Spatzal, T.; Aksoyoglu, M.; Zhang, L. M.; Andrade, S. L. A.; Schleicher, E.; Weber, S.; Rees, D. C.; Einsle, O. Evidence for interstitial carbon in nitrogenase FeMo cofactor. *Science* **2011**, *334*, 940.

8. Umena, Y.; Kawakami, K.; Shen, J.; Kamiya, N. Crystal structure of oxygen-evolving photosystem II at a resolution of 1.9Å. *Nature*. **2011**, 473, 55-61.

9. Kanady, J.; Tsui, E.; Day, M.; Agapie, T. A Synthetic Model of the Mn_3Ca Subsite of the Oxygen-Evolving Complex in Photosystem II. *Science*. **2011**, 333, 733-736.

10. McEvoy, J. P.; Brudvig, G. W. Water Splitting Chemistry of Photosystem II. *Chem. Rev.* **2006**, 106, 4455–4483.

11. Yano, J.; Yachandra, V. Mn_4Ca Cluster in Photosynthesis: Where and How Water is Oxidized to Dioxygen. *Chem. Rev.* **2014**, 114, 4175–4205.

12. Koua, F.; Umena, Y.; Kawakami, K.; Shen, J.R. Structure of Sr-substituted photosystem II at 2.1 Å resolution and its implications in the mechanism of water oxidation. *Proc. Nat. Acad. Sci. USA.* **2013**, 110, 3889-3894.

13. Hendry, G.; Wydrzynski, T. ^{18}O Isotope Exchange Measurements Reveal that Calcium Is Involved in the Binding of One Substrate-Water Molecule to the Oxygen-Evolving Complex in Photosystem II. *Biochemistry*. **2003**, 42, 6209–6217.

14. Herbert, D.; Lionetti, D.; Rittle, J.; Agapie, T. Heterometallic Triiron-Oxo/Hydroxo Clusters: Effect of Redox-Inactive Metals. *J. Am. Chem. Soc*. **2013**, 135, 19075-19078.

15. Tsui, E.; Agapie, T. Reduction potentials of heterometallic manganese–oxido cubane complexes modulated by redox-inactive metals. *Proc. Natl. Acad. Sci. USA*. **2013**, 110, 10084-10088.

16. Tsui, E.; Kanady, J.; Agapie, T. Synthetic Cluster Models of Biological and Heterogeneous Manganese Catalysts for O_2 Evolution. *Inorg. Chem*. **2013**, 52, 13833-13848.

17. Lionetti, D.; Suseno, S.; Tsui, E.; Lu, L.; Stich, T.; Carsch, K.; Neilsen, R.; Goddard, W.; Britt, D.; Agapie, T. Effects of Lewis Acidic Metal Ions (M) on Oxygen-Atom Transfer Reactivity of Heterometallic Mn_3MO_4 Cubane and $Fe_3MO(OH)$ and $Mn_3MO(OH)$ Clusters. *Inorg. Chem*. **2019**, 58, 2336-2345.

18. van Staveren, C.; van Eerden, J.; van Veggel, F.; Harkema, S.; Reinhoudt, D. Cocomplexation of Neutral Guests and Electrophilic Metal Cations in Synthetis Macrocyclic Hosts. *J. Am. Chem. Soc*. **1988**, 110, 4994-5008.

19. Gokel, G. W.; Leevy, W. M.; Weber, M. E. Crown ethers: sensors for ions and molecular scaffolds for materials and biological models. *Chem. Rev.* **2004**, 104, 2723 –2750.

20. Perrin, D. *Ionization Constants of Inorganic Acids and Bases in Aqueous Solution*, Pergamon, Oxford, **1982**.

21. Kumar, A.; Lionette, D.; Day, V.; Blakemore, J. Trivalent Lewis Acidic Cations Govern the Electronic Properties and Stability of Heterobimetallic Complexes of Nickel. *Chem. Eur. J*. **2018**, 24, 141-149.

22. Bard, A.; Parsons, R.; Jordan, J. *Standard Potentials in Aqueous Solution*, M. Dekker, New York, 1985.

23. Groom, C.; Bruno, I.; Lightfoot, M.; Ward, S. The Cambridge Structural Database. *Acta Cryst. Sect. B*. **2016**, 72, 171-179.